

## Elementary electronic excitations in a quasi-two-dimensional electron gas

Jainendra K. Jain and S. Das Sarma

*Department of Physics and Astronomy, University of Maryland, College Park, Maryland 20742*

(Received 4 June 1987)

The complete elementary excitation spectrum for a quasi-two-dimensional electron gas is calculated within the random-phase approximation for both single and multilayer systems. Specific predictions are made for the direct observation via inelastic light scattering of a number of new modes and mode-coupling effects.

The subband structure in semiconductor heterostructures, arising from finite thickness of the quasi-two-dimensional electron gas, gives rise to interesting quantum effects that are completely missed by a purely two-dimensional treatment. The intersubband transitions correspond to charge-density oscillations perpendicular to the plane and there is a collective mode associated with them called the intersubband plasmon.<sup>1</sup> Also, the dispersion of the intrasubband plasmon, whose energy goes as  $\sqrt{q}$  in the long-wavelength limit in two dimensions,<sup>2</sup> itself is affected by the finite thickness and by coupling to higher subbands.<sup>3</sup> These phenomena have been studied in detail.

In this work we study the spin- and charge-density excitations of a quasi-two-dimensional electron gas considering the complete elementary excitation spectrum. We give special emphasis to the coupling of inter- and intrasubband charge-density modes and predict under what conditions the mode-coupling phenomenon can be observed by inelastic light scattering experiments. In a recent publication<sup>4</sup> an experimental manifestation of this coupling has been observed in a single-layer silicon metal oxide semiconductor field-effect transistor (MOSFET) system by a far-infrared transmission experiment. However, our current work is the first detailed theory for this interesting mode-coupling phenomenon. We also feel that inelastic light scattering experiments or Fourier-transform far-infrared spectroscopy on GaAs-Al<sub>x</sub>Ga<sub>1-x</sub>As heterostructures would be a more definitive and cleaner way of observing the resonant coupling since one does not need external stress to achieve resonance. The spin-density excitation spectrum is found to have interesting observable structure not reported earlier. We also consider multicomponent systems with more than one subband occupied. All the calculations are carried out in random-phase approximation (RPA), which has proven to be quite accurate in the past.<sup>5,6</sup>

In order to focus our attention on the physics that we want to address, we make a number of simplifying approximations, none of which, however, affects our results in any essential way. We model the semiconductor quantum well by an infinite square-well potential of width  $L$ , thus ignoring the finite-depth and band-bending effects. This can be remedied to an extent simply by

treating the subband separation as an adjustable parameter. We also ignore (i) coupling to LO phonons, because we shall be concerned with plasmon energies that are quite small compared to LO phonon energy; (ii) final-state or excitonic effects, which are supposed to be small in GaAs-AlGaAs;<sup>7</sup> (iii) exchange-correlation effects; (iv) image-charge effect due to dielectric mismatch at the surface and the interfaces. All these approximations can be systematically relaxed and their net effect on our final results is expected to be less than 10% in the regime we are working in.

The charge-density excitation spectrum is given by the imaginary part of the dynamical polarizability (or, density-density correlation) function,  $D(\mathbf{q}, q_z, \omega)$ :

$$D(q_z) = \int_{-L/2}^{L/2} \int_{-L/2}^{L/2} dz dz' e^{-iq_z(z-z')} D(z, z'), \quad (1)$$

$$D(z, z') = \sum_{i,j,k,l} D_{ij,kl} \xi_i(z) \xi_j(z) \xi_k(z') \xi_l(z'), \quad (2)$$

$$D_{ij,kl} = D_{ij}^0 \delta_{ik} \delta_{jl} + \sum_{m,n} D_{ij}^0 V f_{ij,mn} D_{mn,kl}, \quad (3)$$

$$f_{ij,kl} = \int_{-L/2}^{L/2} \int_{-L/2}^{L/2} dz dz' \xi_i(z) \xi_j(z) e^{-q|z-z'|} \times \xi_k(z') \xi_l(z'), \quad (4)$$

$$D_{ij}^0 = 2 \sum_{\mathbf{k}} \frac{f_j(\epsilon_j(\mathbf{k} + \mathbf{q})) - f_i(\epsilon_i(\mathbf{k}))}{\epsilon_j(\mathbf{k} + \mathbf{q}) - \epsilon_i(\mathbf{k}) - \hbar(\omega + i\gamma)}. \quad (5)$$

All the vectors (i.e., quantities such as  $\mathbf{q}$  appearing with explicit vector signs) are two-dimensional in-plane vectors, whereas  $q_z$  refers to the  $z$  wave vector. The dependence of quantities on wave-vector exchange  $\mathbf{q}$  and energy exchange  $\omega$  is not shown explicitly, for the sake of brevity. Subscripts are the subband indices.  $V f_{ij,kl}$ , with  $V = 2\pi e^2 / \epsilon q$  ( $\epsilon$  is the background static dielectric constant), is the Fourier transform of the Coulomb interaction for the quantum well, and  $\xi_j$  is the wave function for the  $j$ th subband. If only the two lowest subbands are considered, then the only independent  $f$ 's are  $f_{11,11}$ ,  $f_{11,22}$ ,  $f_{22,22}$ ,  $f_{12,12}$ ,  $f_{11,12}$ , and  $f_{22,12}$ . For small  $qL$ , the first three are close to unity whereas the last two are close to zero due to the orthonormality of wave functions. For a symmetric potential well the last two (i.e.,  $f_{11,12}$  and  $f_{22,12}$ ) are strictly zero for arbitrary  $q$ .

$D_{ij}^0$  is the polarizability function for the  $i \rightarrow j$  transition in the absence of Coulomb interactions and is given by expression (5), where  $\epsilon_j(\mathbf{k}) = \hbar E_j + \hbar^2 k^2 / 2m$  is the single-particle energy in the  $j$ th subband, and  $f(\epsilon)$  is the Fermi occupation probability. A finite value of  $\gamma$  (usually 0.1–1.0 meV; we shall take  $\gamma = 0.1$  meV) takes care of scattering by impurities phenomenologically. The integral in (5) can be carried out and if we assume the subbands to be parabolic with the same effective mass,

$$D_{ij}^0 = -\frac{m}{\pi \hbar^2} \left[ \frac{k_{F,j}}{q} [a_{+j} - (a_{+j}^2 - 1)^{1/2}] - \frac{k_{F,i}}{q} [a_{-i} - (a_{-i}^2 - 1)^{1/2}] \right],$$

$$a_{\pm k} = \frac{\omega - E_j + E_i + i\gamma}{qv_{F,k}} \pm \frac{q}{2k_{F,k}}, \quad (6)$$

where  $k_F$  and  $v_F$  denote Fermi wave vector and Fermi velocity, respectively, and the square root of a complex quantity is always chosen to be the one with positive imaginary part. For  $i = j$ ,  $D_{ij}^0$  reduces to the well-known form<sup>2</sup> which can be approximated by  $n_i q^2 / m \omega^2$  for  $\omega \gg qv_{F,i}$ . For  $i \neq j$  and  $q \rightarrow 0$ ,  $D_{ij}^0$  can be approximated by  $(n_j - n_i) / (\hbar E_{ji} - \hbar \omega)$ , where  $E_{ji} = E_j - E_i$ . For our numerical calculations, however, we shall use the exact expression (6), which is important for the spin-density excitation spectrum as well as for studying the Landau damping of charge-density excitations. Equation (3) takes dynamic screening into account by the standard method of summing up the ring diagrams. The spin-density excitations, on the other hand, are not screened because Coulomb interactions cannot flip the electron spin. Therefore the summation in Eq. (3) is omitted while calculating the spin-density excitation spectrum, which is given by  $\text{Im}D(\mathbf{q}, \omega, q_z)$ . Both charge- and spin-density excitation spectra can be observed by inelastic light scattering by looking at the scattered photon that has polarization in the same or perpendicular direction as the incident photon.<sup>8</sup>

Let us consider only two subbands, denoted by subscripts 1 and 2. By energy-momentum conservation it is clear that spin-density excitations with in-plane wave vector  $\mathbf{q}$  are allowed only within the energy ranges  $[0, qv_{F,1}]$  and  $[E_{21} - qv_{F,1}, E_{21} + qv_{F,1}]$ , where we have assumed that  $q \ll k_F$ . The spectrum is shown in Fig. 1 for two different values of  $q_z L$ , and has peaks near the boundaries  $qv_{F,1}$ ,  $qv_{F,2}$ , and  $E_{21} \pm qv_{F,1}$ . For the parameters we have chosen, the first two peaks are indistinguishable. The relative weight in the intra- and intersubband transitions depends on the value of  $q_z L$ . For  $q_z L \rightarrow 0$  the weight in the intersubband spectrum is zero—as is intuitively obvious, because the intersubband transitions correspond to a charge disturbance in the  $z$  direction—and it increases as  $q_z L$  increases.

Now we come to the charge-density excitation spectrum. It has peaks at the poles of  $D_{ij,mn}$  which occur when the determinant of  $D_{ij}^0 V f_{ij,mn} - \delta_{ij,mn}$  vanishes. If only the lowest subband is occupied, then this  $3 \times 3$  determinant (because  $ij$  and  $mn$  can take only three values: 11, 12, 21) vanishes when

$$D_{11}^0 V f_{11,11} = 1, \quad (7)$$

or when

$$(D_{12}^0 + D_{21}^0) V f_{12,12} = 1. \quad (8)$$

Equation (7) gives the dispersion of the intrasubband plasmon which reduces to the correct 2D limit<sup>2</sup> for  $f_{11,11} = 1$ . Equation (8) is the dispersion of the intersubband plasmon<sup>1</sup> which, with the approximate form of  $D_{ij}^0$ , becomes

$$\omega^2 = E_{21}^2 + 2E_{21} V f_{12,12} (n_1 - n_2) / \hbar. \quad (9)$$

( $n_2$  is zero at the moment.) The intersubband plasmon energy is shifted upwards of the subband spacing  $E_{21}$  because of depolarization field effects.

When both the subbands are occupied, the intersubband plasmon is still given by Eq. (8), and the two intrasubband modes are coupled as

$$\begin{vmatrix} D_{11}^0 V_{11,11} - 1 & D_{11}^0 V_{11,22} \\ D_{22}^0 V_{11,22} & D_{22}^0 V_{22,22} - 1 \end{vmatrix} = 0.$$

With the approximate form  $D_{ii}^0 = n_i q^2 / m \omega^2$ , this equation can easily be solved for two coupled intrasubband plasmons. Rather than writing down the dispersions, we point out that one of the plasmons has linear dispersion in  $q$  but is strongly Landau damped, whereas the dispersion of the other plasmon is approximately given by Eq. (7) with the assumption that all the electrons occupy the lowest subband only. This is shown in Fig. 2. Thus Eq. (7), which includes the finite-thickness effect through  $f_{11,11}$  but ignores all subbands except the lowest one, is a good approximation for the intrasubband plasmon even when more than one subband is occupied.

Note that until now the inter- and intrasubband charge-density modes have been completely uncoupled

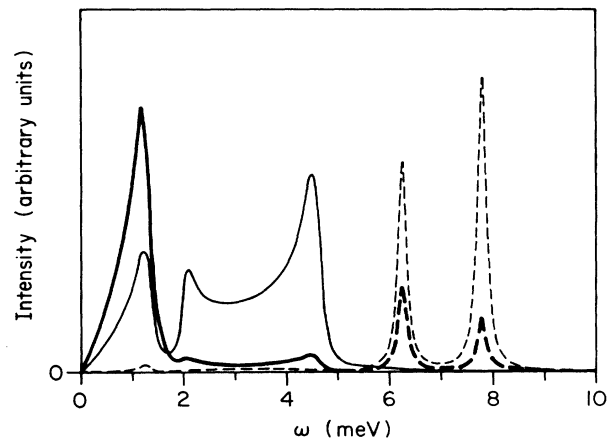


FIG. 1. Spin-density spectrum (solid lines) and charge-density spectrum (dashed lines) for  $q_z L = 4.0$  (thin lines) and  $q_z L = 1.0$  (thick lines). All spectra are drawn on the same scale. The sample parameters are the same as in Fig. 3,  $q = 7 \times 10^4 \text{ cm}^{-1}$ ,  $\gamma = 0.1 \text{ meV}$ .

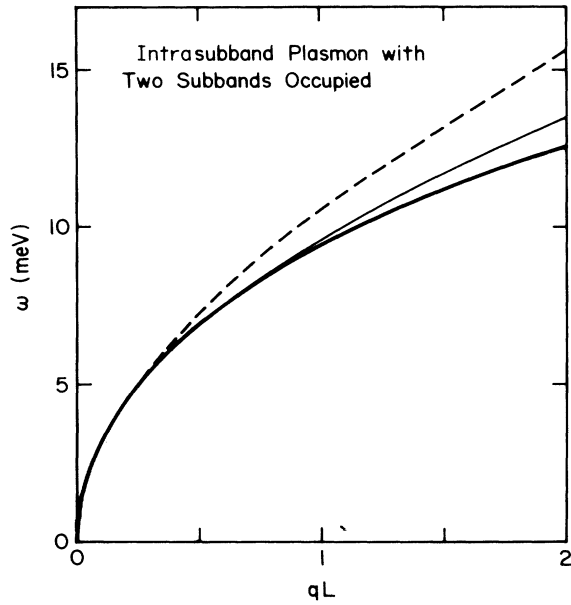


FIG. 2. Dispersion of the intrasubband plasmon for the sample of Fig. 3. Two subbands are occupied. The thick solid line is the correct RPA dispersion assuming that there is no coupling with the intersubband plasmon. The thin line is the finite-thickness approximation given by Eq. (7). The dashed line is the dispersion of the pure two-dimensional plasmon, which is given by Eq. (7) with  $f_{11,11} = 1$ .

as the Coulomb matrix elements  $f_{11,12}$  and  $f_{22,12}$  are identically zero because of the symmetric nature of the quantum well around its midpoint. As  $f_{11,13}$  and  $f_{33,13}$  are not zero, there is a coupling between the intrasubband plasmon and  $1 \rightarrow 3$  intersubband plasmon, but it would be difficult to see this experimentally because usually the  $1 \rightarrow 3$  intersubband plasmon has fairly high energy and it becomes Landau damped (by entering the intersubband single-particle excitation regime) much before the intrasubband plasmon may get close to it. In actual experimental situations, however, the two interfaces of a quantum well are not identical and charge accumulates more near one of them. We simulate this asymmetry in our model by elevating one-half of the quantum well by a small amount of energy, as shown in Fig. 3. We then solve numerically for the eigenvalues and the eigenfunctions. To make an experimental observation of the coupling possible, it is desirable to have a low-energy intersubband plasmon and a quickly rising intrasubband plasmon. This can be achieved by making the quantum well quite thick so that  $E_{21}$  is small, and having a high electron density. Notice that once the second subband starts to fill up, the intersubband plasmon energy does not change appreciably (in fact, within our model it remains constant). We choose the layer thickness  $L = 700 \text{ \AA}$ , electron density  $n = 9.0 \times 10^{11} \text{ cm}^{-2}$ , and the potential step at the midpoint as 0.5 meV.

The dispersions of the inter- and intrasubband modes are obtained numerically and shown in Fig. 3. Wave-

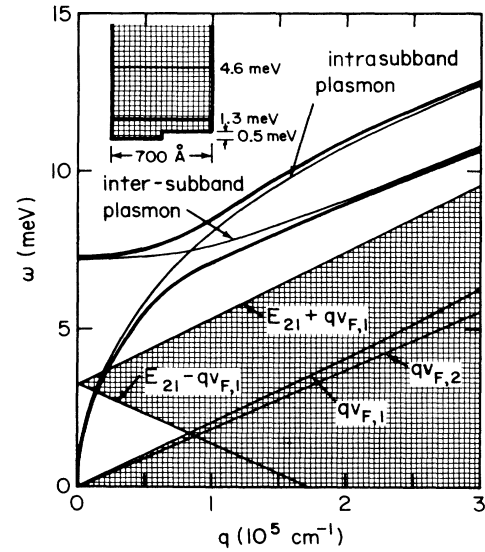


FIG. 3. Resonant coupling of the inter- and intrasubband plasmons is shown. The coupled modes are shown by thick lines and the uncoupled modes by thin ones. The shaded area denotes the region where single-particle excitations are allowed. The asymmetric semiconductor quantum well is shown in the inset with its quantized energy levels. The various parameters are as follows: effective mass equals  $0.07m_e$ ,  $n = 9 \times 10^{11} \text{ cm}^{-2}$ ,  $n_1 = 5 \times 10^{11} \text{ cm}^{-2}$ ,  $n_2 = 4 \times 10^{11} \text{ cm}^{-2}$ ,  $E_{21} = 3.3 \text{ meV}$ , background dielectric constant  $\epsilon = 13.1$ .

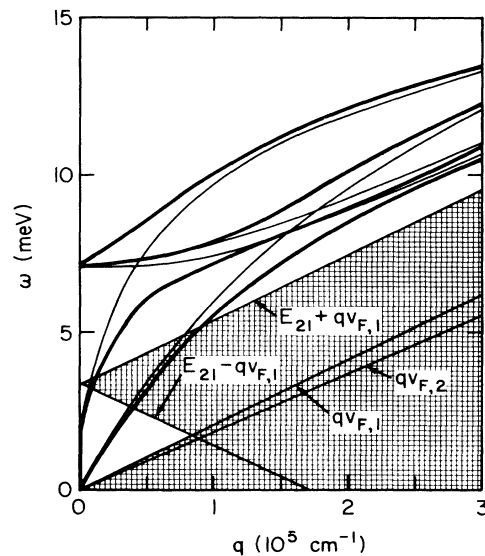


FIG. 4. Dispersion of the plasmons for a system with two quasi-two-dimensional electron layers. Each of the layers consists of the quantum well shown in Fig. 3, and their midpoints are separated by  $940 \text{ \AA}$ . There are two intersubband modes and two intrasubband modes. The coupled modes are shown by thick lines and the uncoupled modes by thin ones. Shaded region is the single-particle excitation regime.

vector exchange up to  $3 \times 10^5 \text{ cm}^{-1}$  is possible in Raman experiments. To see the effect of coupling clearly, the dispersions are also plotted for the uncoupled case, where the coupling is eliminated by explicitly putting  $f_{11,12}$  and  $f_{22,12}$  equal to zero. The coupling results in a sizable splitting of the energies at the resonance point. The correction away from the resonance point is also non-negligible. In particular, the intersubband plasmon becomes strongly  $q$  dependent even for small  $q$  (also see Fig. 4). At the resonance point, the Coulomb matrix elements  $f_{11,11}$ ,  $f_{11,22}$ , and  $f_{22,22}$  are close to 0.9 and  $f_{12,12}$ ,  $f_{11,12}$ , and  $f_{22,12}$  are of order 0.06. Also notice that the intrasubband plasmon is not damped inside the intersubband single-particle excitation regime, because a charge-density wave parallel to the  $xy$  plane cannot excite particles across the subbands. For  $q = 7 \times 10^4 \text{ cm}^{-1}$ , the charge-density excitation spectrum is shown in Fig. 1 for two different values of  $q_z L$ . The relative intensity of the modes depends on  $q_z L$  and for  $q_z L \rightarrow 0$  there is vanishing weight at the intersubband plasmon energy.

Now let us briefly consider systems with multiple quantum wells. For the sake of clarity, and also because the physics becomes quite transparent, we consider only two layers with their midpoints separated by 940 Å. (For a larger number of layers the calculation is straightforward and the results are what one would expect on the basis of this two-layer calculation.) The plasmons are obtained after generalizing Eqs. (1)–(4) and are plotted in Fig. 4 along with the uncoupled dispersions.

There are now two intersubband and two intrasubband modes. For an infinite number of layers<sup>9</sup> there would be bands of inter- and intrasubband plasmons. For a finite superlattice, the discrete intrasubband modes<sup>10</sup> have been observed experimentally,<sup>6</sup> and although the energy separation of the discrete intersubband modes is not as large, by closely looking at the Raman spectra their resolution may be possible. The coupling between inter- and intrasubband modes is clearly visible. In fact, superlattices are a better candidate for observing this coupling because they have discrete plasmons with energies higher than the intrasubband plasmon of a single layer.

In conclusion, we have outlined the conditions for experimental observation of the resonant mode coupling of inter- and intrasubband plasmons. These are (i) anisotropy of the quantum well, (ii) small  $E_{21}$ , (iii) large two-dimensional density of electrons, and (iv) large  $q_z L$  (which can be achieved, for example, in a backscattering geometry). We have indicated the possibility of the observation of discrete intersubband coupled-layer plasmons, and of two peaks at  $E_{21} \pm qv_F$  in the intersubband spin-density excitation spectrum for large  $q_z L$ . We have also described systems with multiple subband occupancy.

This work is supported by the Army Research Office. The authors are grateful to the University of Maryland Computer Center for their support.

- 
- <sup>1</sup>D. A. Dahl and L. J. Sham, *Phys. Rev. B* **16**, 651 (1977); A. C. Tselis and J. J. Quinn, *ibid.* **29**, 3318 (1984); P. Kneschaurek, A. Kamgar, and J. F. Koch, *ibid.* **14**, 1610 (1976); D. Heitmann, J. P. Kotthaus, and E. G. Mohr, *Solid State Commun.* **44**, 715 (1982); A. Pinczuk, J. M. Worlock, H. L. Störmer, R. Dingle, W. Wiegmann, and A. C. Gossard, *ibid.* **36**, 43 (1980); R. Sooryakumar *et al.*, *Phys. Rev. B* **31**, 2578 (1981). For a more complete list, see T. Ando, A. B. Fowler, and F. Stern, *Rev. Mod. Phys.* **54**, 437 (1982).
- <sup>2</sup>F. Stern, *Phys. Rev. Lett.* **18**, 546 (1967).
- <sup>3</sup>S. Das Sarma, *Phys. Rev. B* **29**, 2334 (1984).
- <sup>4</sup>S. Oelting, D. Heitmann, and J. P. Kotthaus, *Phys. Rev. Lett.* **56**, 1846 (1986).
- <sup>5</sup>C. C. Grimes and G. Adams, *Surf. Sci.* **58**, 292 (1976); S. J. Allen, D. C. Tsui, and R. A. Logan, *Phys. Rev. Lett.* **38**, 980 (1977); T. N. Theis, J. P. Kotthaus, and P. J. Stiles, *Solid State Commun.* **26**, 603 (1978); D. Olego, A. Pinczuk, A. C. Gossard, and W. Wiegmann, *Phys. Rev. B* **25**, 7867 (1982); J. K. Jain and P. B. Allen, *Phys. Rev. Lett.* **54**, 947 (1985); *Phys. Rev. B* **32**, 997 (1985).
- <sup>6</sup>A. Pinczuk, M. G. Lamont, and A. C. Gossard, *Phys. Rev. Lett.* **56**, 2092 (1986); G. Fasol, N. Mestres, H. P. Hughes, A. Fischer, and K. Ploog, *ibid.* **56**, 2517 (1986).
- <sup>7</sup>T. Ando and S. Mori, *J. Phys. Soc. Jpn.* **47**, 1518 (1979).
- <sup>8</sup>E. Burstein, A. Pinczuk, and D. L. Mills, *Surf. Sci.* **98**, 451 (1980).
- <sup>9</sup>A. L. Fetter, *Ann. Phys. (NY)* **88**, 1 (1974); D. Grecu, *Phys. Rev. B* **8**, 1958 (1973); S. Das Sarma and J. J. Quinn, *ibid.* **25**, 7603 (1982).
- <sup>10</sup>J. K. Jain and P. B. Allen, *Phys. Rev. Lett.* **54**, 2437 (1985).